ARTICLE

doi:10.1016/S1525-0016(03)00098-4

Recombinant Adeno-associated Virus Serotype 4 Mediates Unique and Exclusive Long-Term Transduction of Retinal Pigmented Epithelium in Rat, Dog, and Nonhuman Primate after Subretinal Delivery

Michel Weber,[1,2] Joseph Rabinowitz,[3] Nathalie Provost,[1] Hervé Conrath,[1,2] Sébastien Folliot,[1] Delphine Briot,[1] Yan Chérel,[4] Pierre Chenuaud,[1] Jude Samulski,[3] Philippe Moullier,[1] and Fabienne Rolling[1,*]

[1]*Laboratoire de Thérapie Génique, INSERM ERM01-05, CHU-Hotel DIEU, Bat. J. Monnet, 30 Avenue J. Monnet, 44035 Nantes Cedex 01, France*
[2]*Service d'Ophtalmologie, CHU-Hotel DIEU, 1 Place Alexis Ricordeau, 44000 Nantes, France*
[3]*Gene Therapy Center and Department of Pharmacology, University of North Carolina, Chapel Hill, North Carolina 27599*
[4]*Laboratoire d'Anatomie Pathologique, INRA UR 703, Ecole Nationale Vétérinaire, 44000 Nantes, France*

**To whom correspondence and reprint requests should be addressed. Fax: (33) 240087491. E-mail: frolling@sante.univ-nantes.fr.*

We previously described chimeric recombinant adeno-associated virus (rAAV) vectors 2/4 and 2/5 as the most efficient vectors in rat retina. We now characterize these two vectors carrying the CMV.*gfp* genome following subretinal injection in the Wistar rat, beagle dog, and cynomolgus macaque. Both serotypes displayed stable GFP expression for the duration of the experiment (6 months) in all three animal models. Similar to the AAV-2 serotype, AAV-2/5 transduced both RPE and photoreceptor cells, with higher level of transduction in photoreceptors, whereas rAAV-2/4 transduction was unambiguously restricted to RPE cells. This unique specificity found conserved among all three species makes AAV-2/4-derived vectors attractive for retinal diseases originating in RPE such as Leber congenital amaurosis (RPE65) or retinitis pigmentosa due to a mutated mer*tk* gene. To provide further important preclinical data, vector shedding was monitored by PCR in various biological fluids for 2 months post-rAAV administration. Following rAAV-2/4 and -5 subretinal delivery in dogs ($n = 6$) and in nonhuman primates ($n = 2$), vector genome was found in lacrymal and nasal fluids for up to 3–4 days and in the serum for up to 15–20 days. Overall, these findings will have a practical impact on the development of future gene therapy trials of retinal diseases.

Key Words: AAV vectors, serotypes, retina, gene transfer, tropism, GFP, rat, dog, primate

INTRODUCTION

Recombinant adeno-associated virus (rAAV)-2 vectors are capable of efficient and prolonged transgene expression in a number of tissues and have been used to deliver therapeutic genes to correct defects in animal models of various human disorders [1–8]. More recently, seven other rAAV serotypes (AAV-1, -3, -4, -5, -6, -7, and -8) have been isolated and cloned [9–14]. A number of *in vivo* studies showed that these new serotypes displayed tissue preference and, therefore, improved safety [9,15–18]. However, so far, none of the new serotypes was reported to exhibit a cell-type restriction in a given organ with a conserved tropism among mammalians including a nonhuman primate. In the retina, following subretinal delivery, AAV-2 vectors transduced retinal pigmented epithelium and photoreceptor cells [19–21] and were successful in delivering ribozymes, photoreceptor genes, and neurotrophic factors in mice and rat models of retinal degeneration [22–26]. Visual function was restored in a canine model of childhood blindness using a rAAV-2 carrying a wtRPE65 gene, providing critical preclinical data supporting these vectors for human applications [27]. We and others studied rAAV chimeric serotypes in which the vector is flanked by AAV-2 ITRs but encapsidated in an AAV-1, -2, -3, -4, or -5 shell [28–30]. We showed that their subretinal delivery resulted in a quantitative transgene expression hierarchy with rAAV-4 and -5 capsids being the most efficient.

The present study was designed to evaluate the rAAV-4

1525-0016/03 $30.00

serotype delivered in the subretinal space of the rat, the dog, and a nonhuman primate. Comparative evaluation with serotype 5 was done in rat and canine models. We believe that rAAV-mediated gene transfer in the eye of large animals is highly relevant with respect to future clinical development as it is anatomically more similar to the human eye than either the mouse or the rat counterpart. Also, surgical procedures for vector delivery are similar. Therefore, studying vector shedding in this context provides additional important preclinical information.

RESULTS

Subretinal Delivery of rAAV-2/4.CMV.*gfp* and rAAV-2/5.CMV.*gfp* in Rats

We performed subretinal injections of rAAV-2/4.CMV.*gfp* and rAAV-2/5.CMV.*gfp* (4×10^{12} and 2×10^{12} vector genome (vg)/ml corresponding to 8×10^{9} and 4×10^{9} vg/injection, respectively) on six Wistar rats ($n = 3$ for each serotype). As previously observed, fluorescent imaging in live animals displayed a different pattern between rAAV-2/4 and rAAV-2/5 [28], i.e., speckled GFP spots for rAAV-2/4 (Fig. 1A), whereas rAAV-2/5 displayed in addition a uniform and homogeneous GFP signal (Fig. 1B). In retina flat mounts, using a fluorescence inverted microscope, rAAV-2/4-mediated gene expression was restricted to the sclera/choroid/ retinal pigmented epithelium (RPE) layer (Fig. 1C) and more specifically to RPE cells (Fig. 1G). No signal was ever detected in the neuroretina layer (Figs. 1E and 1I). Conversely, rAAV-2/5-injected retina showed GFP signal in both the sclera/choroid/RPE layer and the neuroretina (Figs. 1D and 1F), namely, the RPE cells and the photoreceptors (Figs. 1H and 1J).

Subretinal Delivery of rAAV-2/4.CMV.*gfp* and rAAV-2/5.CMV.*gfp* in Dogs

We performed subretinal injection of rAAV-2/4.CMV.*gfp* and rAAV-2/5.CMV.*gfp* via a transvitreal route within the tapetal retina of six dogs (D1–D3 and D4–D6, respectively). We chose the tapetal retina because RPE cells are not pigmented in this region. D1 and D4 contralateral eyes received saline injection (vehicle) alone. Retinas had all flattened by 24 h postinjection (p.i.) and no inflammatory response was detected by fundus photography (data not shown). The transduced area seen by fluorescence exactly matched the retinal detachment created by the injection (Fig. 2). No fluorescence was detectable in the vehicle-injected eyes (data not shown).

In rAAV-2/4.CMV.*gfp* animals, we detected weak GFP expression first 15 days p.i. and it gradually increased to reach a maximum level at ≈60 days (Figs. 2A, 2C, 2E, 2G, and 2I). Conversely, in rAAV-2/5.CMV.*gfp* animals, GFP expression was rapidly detected 3 days p.i. and then, similar to rAAV-2/4.CMV.*gfp,* the signal gradually increased to reach a maximum level at ≈60 days (Figs. 2B, 2D, 2F, 2H, and 2J). We monitored retinal morphology and GFP expression in D1, D3, D4, and D6 by color fundus photographs for up to 6 months and they showed no abnormalities with a stable level of GFP expression (data not shown).

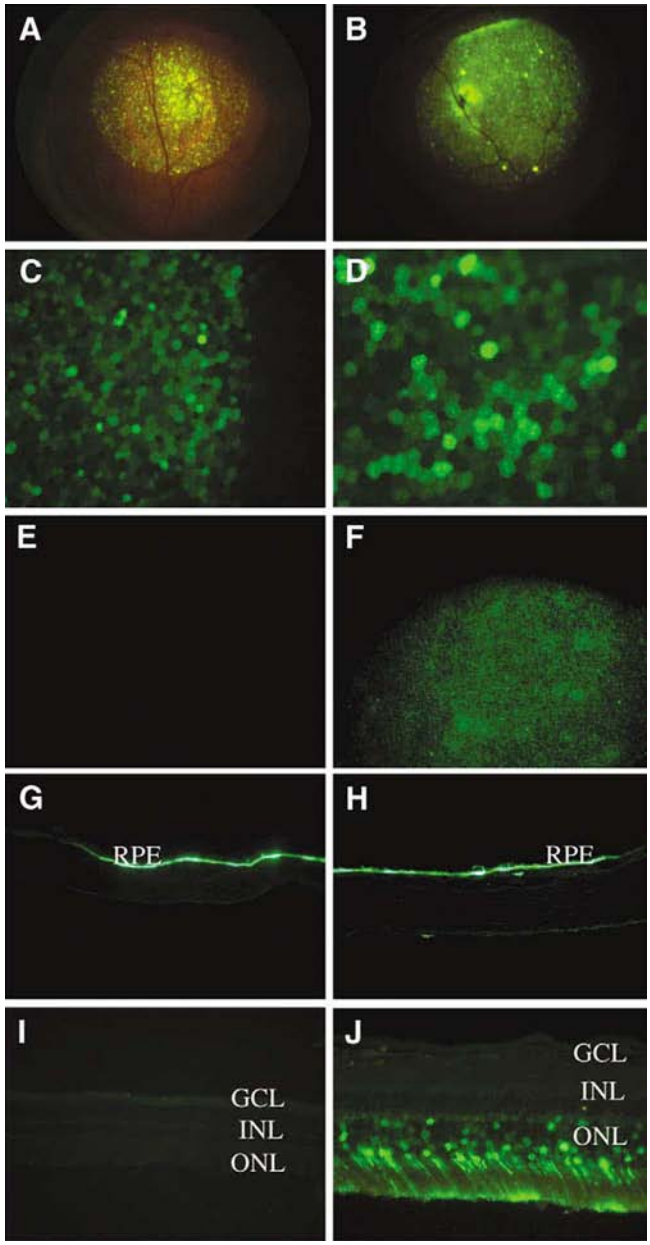

FIG. 1. Rat model. Rats were injected with rAAV-2/4.CMV.*gfp* (A, C, E, G, and I) and rAAV-2/5.CMV.*gfp* (B, D, F, H, and J) and analyzed 30 days p.i. (A and B) Fluorescence retinal imaging. (C and D) Sclera/choroid/RPE and (E and F) neuroretina flat mounts. (G and H) Sections from sclera/choroid/RPE and (I and J) neuroretina examined under an inverted fluorescence microscope. RPE, retinal pigmented epithelium; ONL, outer nuclear layer; INL, inner nuclear layer; GCL, ganglion cell layer.

Two months p.i., retina flat mounts were obtained

doi:10.1016/S1525-0016(03)00098-4

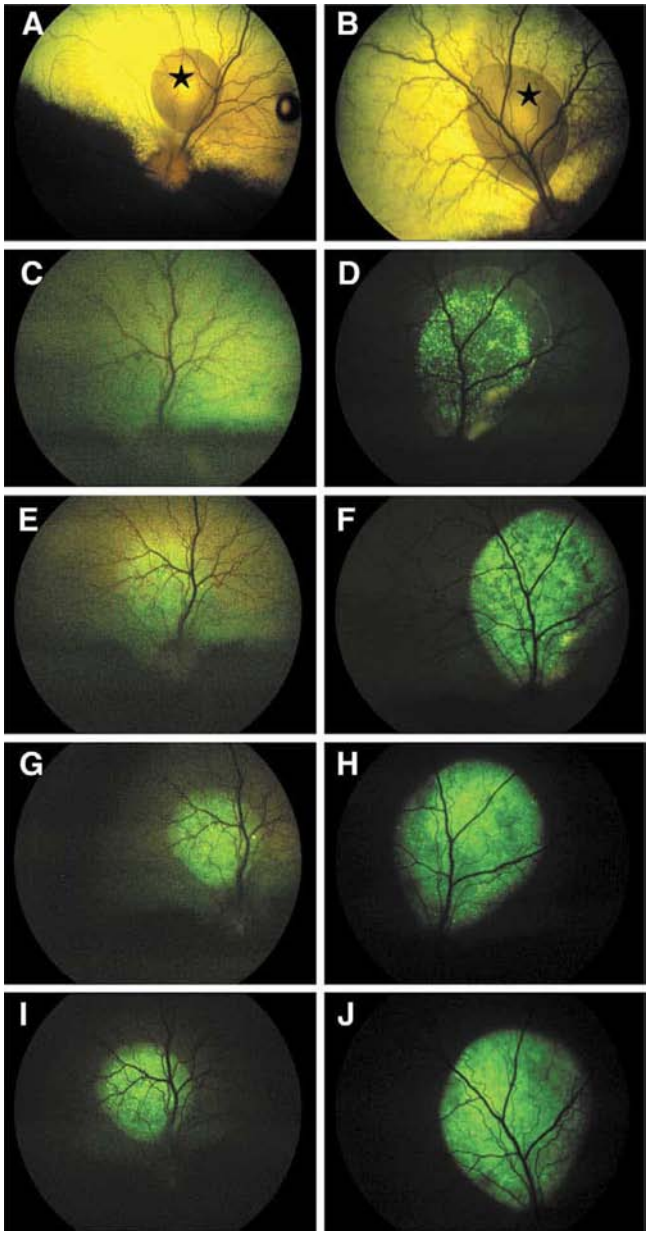

FIG. 2. Dog model. Live fluorescent retinal imaging at different time intervals (3, 15, 30, and 60 days p.i.) in two dogs: D1 injected with rAAV-2/4.CMV.*gfp* (A, C, E, G, and I) and D4 with rAAV-2/5.CMV.*gfp* (B, D, F, H, and J). (★) Retinal detachment created by the subretinal injection (A, B).

from D2 and D5 (rAAV-2/4 and rAAV-2/5, respectively). Choroid/RPE layers were separated from the neuroretina (Figs. 3A and 3B). Using an inverted fluorescence microscope, we found the GFP signal to be restricted to the choroid/RPE layer in D2 (Fig. 3C) and more specifically to the RPE cells after flat-mount sectioning (Fig. 3E). Indeed, no signal could be detected in the neuroretina (Figs. 3D and 3F). Conversely in D5, GFP expression was detected in both the choroid/RPE and the neuroretina flat mounts (Figs. 3G and 3H), namely in RPE and in photoreceptors (Figs. 3I and 3J). There was no RPE atrophy nor cellular infiltration in both D2 and D5.

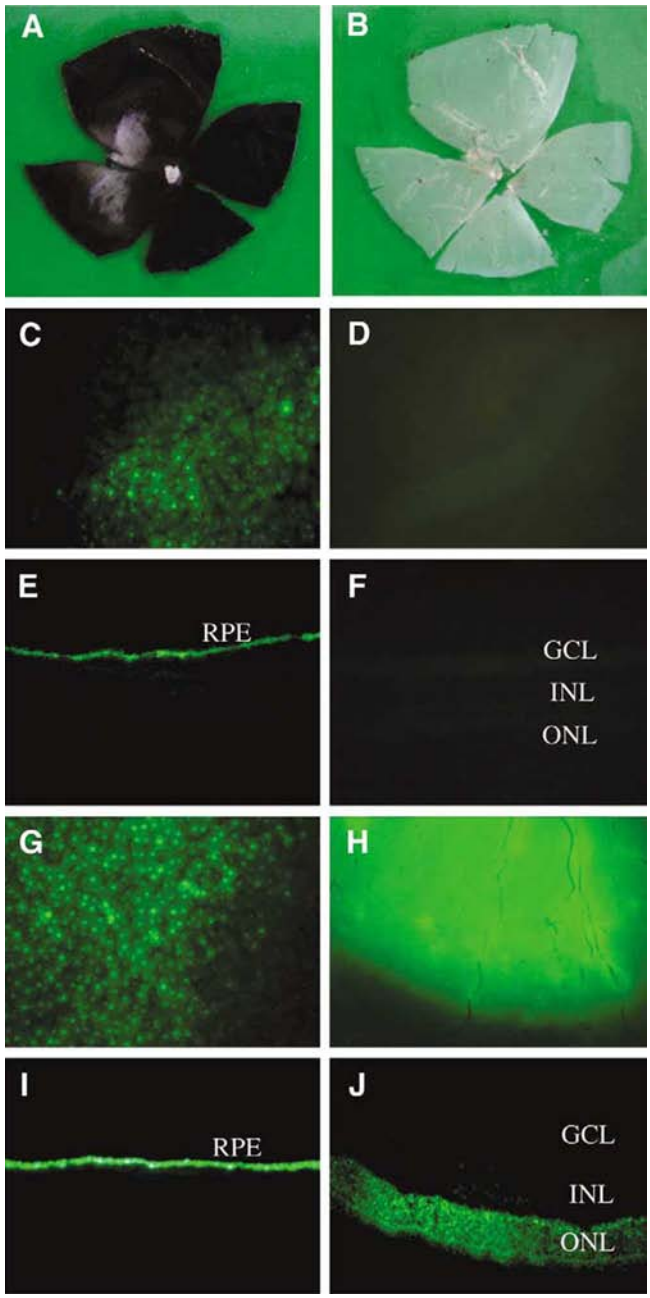

FIG. 3. Dog model. Flat mounts were obtained 2 months p.i. from two dogs: D2 injected with rAAV-2/4.CMV.*gfp* (C, D, E, and F) and D5 with rAAV-2/5.CMV.*gfp* (G, H, I, and J). Choroid/RPE (A) and neuroretina (B) layers were separated. Choroid/RPE (C, E, G, and I) and neuroretina (D, F, H, and J) flat mounts and sections were examined under an inverted fluorescence microscope. See legend to Fig. 1 for RPE, ONL, INL, and GCL.

As in rodents, the results demonstrated that an accurate subretinal injection of rAAV-2/4 vector in dogs leads to unique and exclusive transduction of RPE cells as opposed to the rAAV-2/5 vector for which transgene was expressed both in RPE and in photoreceptor cells.

Subretinal Delivery of rAAV-2/4.CMV.*gfp* in Nonhuman Primates

To test the tropism of the rAAV-2/4 vector in a relevant preclinical animal model, we performed subretinal injection of 40 and 120 μl of rAAV-2/4.CMV.*gfp* via a transvitreal route in Mac1 and Mac2, resulting in retinal detachment outside and within the macula, respectively (Fig. 4). Similar to the canine model, the rAAV-2/4 vector resulted in a detectable GFP signal ≈14 days p.i. in both animals with a maximum expression level ≈60 days p.i. (Fig. 4). While the GFP signal was homogeneous over the targeted area in Mac1 (Figs. 4C, 4E, 4G, and 4I) Mac2 displayed a less intense GFP signal within the macula (Figs. 4D, 4F, 4H, and 4J). Noticeably, compared with live fluorescence imaging obtained in rAAV-2/4.CMV.*gfp*-treated dogs, the GFP signal was less intense in both macaques. This result is not surprising since in primates, RPE cells are strongly pigmented resulting in partial fluorescence quenching. We obtained retinal flat mounts from Mac2 65 days p.i. During the dissection, the choroïd/RPE layer was separated from the neuroretina. However, during this process, pigmented RPE cells located between the two vascular arcades did not detach easily from the neuroretina as evidenced by the presence of RPE pigmentation on the neuroretina (Figs. 4K and 4L). This technical handicap was also observed on uninjected primate eyes and, therefore, was not attributed to the vector or the injection itself (data not shown). As a consequence, GFP signal was observed on both choroid/RPE and neuroretina flat mounts (Figs. 4M and 4N). However, the GFP signal clearly displayed the typical hexagonal shape of RPE cells on both flat mounts. We found no fine pixelized signal in the neuroretina, suggesting that only RPE cells were actually transduced. The signal observed in the neuroretina flat mount could be due either to entire transduced RPE cells or transduced RPE cell microvilli still attached to the photoreceptor outer segments, or both. In support of this, neuroretina sections displayed a pigmented layer that corresponded to residual attached RPE microvilli (Fig. 5A). The only detectable fluorescence signal in the neuroretina was from transduced RPE microvilli (Fig. 5B) and no GFP signal could be detected in the outer nuclear layer or in the photoreceptor outer segments layer. Furthermore, RPE cells were expressing GFP in the choroid/RPE layer (Figs. 5C and 5D). As in rodents and dogs, our results demonstrated that an accurate subretinal injection of rAAV-2/4 vector in macaque led to unique and exclusive transduction of RPE cells.

Vector Shedding after Subretinal Delivery of rAAV in Dog and Nonhuman Primate

To provide additional preclinical data from large animal models, we looked for vector shedding after rAAV delivery in the subretinal space of dogs D1 through D6 and primates Mac1 and Mac2. We used PCR to detect rAAV vector genome in several body fluids (Table 1). We first evaluated the sensitivity of the assay by incubating a known number of viral particles with saline before extracting the DNA as described [31]. The results indicated that a threshold of 10^3 to 10^4 vg particles could be detected (Fig. 6A). We collected serum, lacrymal, and nasal samples from 15 min to 2 months p.i. and analyzed them by PCR to detect the *gfp* DNA. Vector DNA could be detected in the serum as soon as 15 min after rAAV administration and up to 25 days in some instances (Fig. 6B and Table 1). For lacrymal and nasal fluids, viral genome was also detected as soon as 15 min and up to 4 days p.i. (Fig. 6B and Table 1). Overall, the important finding is that rAAV vector was shed in various biological fluids in seven of eight large animals using a clinically relevant surgical procedure and an accurate subretinal delivery (Table 1).

Discussion

This study showed that the type 4 AAV capsid allows exclusive and stable transduction of RPE cells after subretinal delivery, at least with a CMV-driven transgene. This is a unique feature conserved among rodent, canine, and nonhuman primate models. None of the other rAAV serotypes provided such unambiguous specificity [28–30]. Therefore, rAAV-2/4 represents an important candidate vector for therapy of RPE-specific genetic diseases such as retinitis pigmentosa due to a mutated mer*tk* gene [32] and Leber congenital amaurosis [33,27]. In the mouse central nervous system, rAAV-4 was also found to restrict transgene expression to the ependymal cells [17]. This suggest that RPE and ependymal cells may share a common receptor and/or coreceptor. Of note, a less efficient transduction was obtained in the macula area of Mac2. This unexplained observation suggested that additional primates are required to assess further the transduction efficiency within the macula region.

The difference in the onset of transgene expression between rAAV-2/4 (≈15 days) and rAAV-2/5 (≈3 days) vector in the canine model might be due to only one cell type (i.e., RPE) being transduced vs two (i.e., RPE and photoreceptors). The GFP signal may have been higher when both cell types expressed the transgene. An alternative explanation is that rAAV-2/5-mediated transduction was more efficient and provided higher copy number per diploid genome, resulting in faster transgene detection. In any case, maximal transgene expression occurred ≈60 days p.i. in all dogs and macaques. This pattern is shared by the nonchimeric AAV-2 vector [34–37], suggesting

doi:10.1016/S1525-0016(03)00098-4

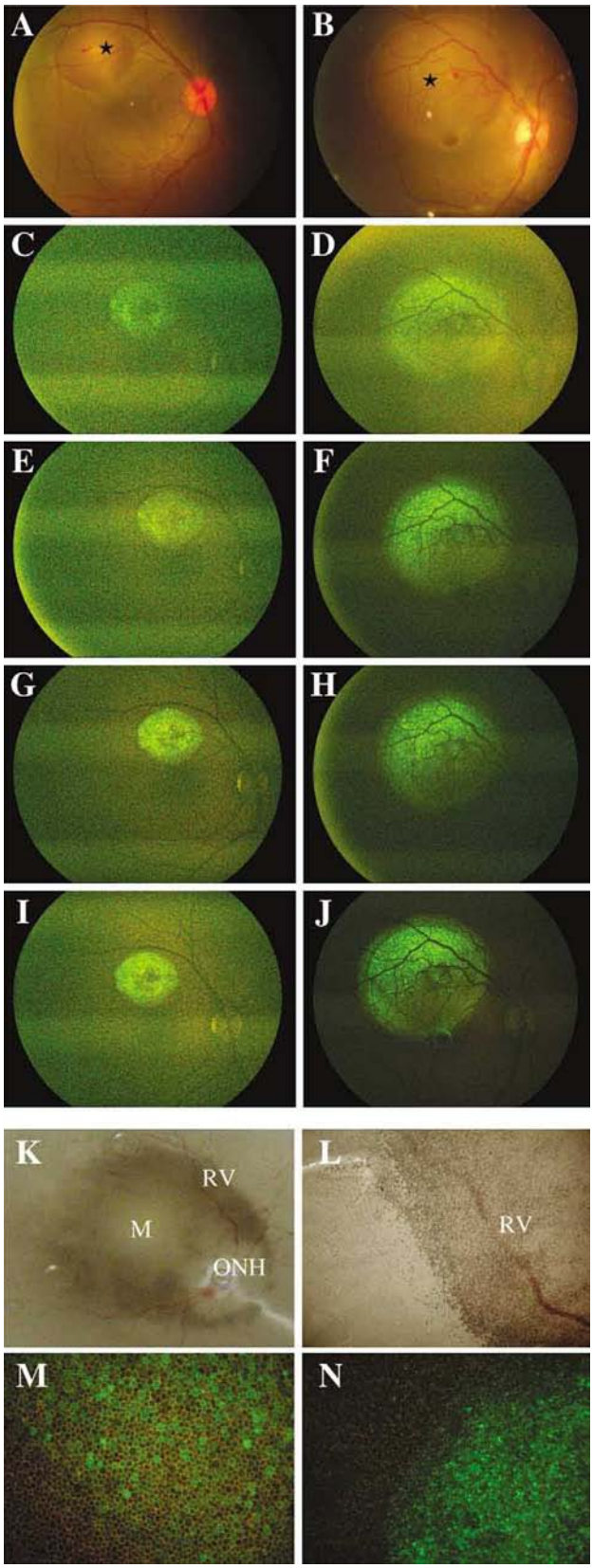

that it is linked to the AAV-2 ITR biology [38–40]. This may be an advantage of the chimeric rAAV vectors over the nonchimeric ones since the AAV-2 ITR-flanking vectors are, so far, the most characterized in preclinical and clinical trials [41,42].

Another important finding in the present study is the discovery of shedding of the rAAV vector immediately and up to several weeks after delivery using a clinically relevant surgical approach. Shedding in lacrymal and nasal fluids was not unexpected because of the transvitreal approach used. However, it remains difficult to explain the presence of the vector in the serum for so long in seven of eight animals. Whether it is possible that noninfectious rAAV vectors trapped in the subretinal space are slowly released to the highly vascularized choroïd remains to be investigated. This finding is in contrast to intramuscular delivery of rAAV-2 vectors of which detection in the sera lasted for only 2days p.i. in factor IX-deficient patients [41] and for 6 days in nonhuman primates [31].

Overall, this study provides evidence that exclusive targeting of the RPE cells is now possible using the rAAV-4 serotype in the rat, dog, and primate, making it an optimal candidate for future clinical trials for Leber congenital amaurosis. However, safety concerns are raised, which will require additional long-term studies in large animal models.

MATERIAL AND METHODS

rAAV-2/4 and rAAV-2/5 vectors. Recombinant AAV-2/4 and -2/5 vectors carried a CMV.*gfp* genome flanked by AAV-2 ITRs encapsidated in an AAV-4 and -5 shell, respectively. AAV-2/4 and AAV-2/5 vectors were produced as previously described [28,43]. The rAAV titers were determined by dot blot and expressed as vector genome/ml [44]. They were 4×10^{12} and 2×10^{12} vg/ml for rAAV-2/4 and rAAV-2/5, respectively.

Subretinal injection. For rat, anesthesia, surgical procedures, and postsurgery care were performed as described previously [45]. Dogs and primates were purchased from the Centre d'Elevage du Domaine des Souches, Mezilles, and BioPrim, Baziège, France, respectively. All animals were cared for in accordance with the ARVO statement for the use of animals in ophthalmic and vision research. Subretinal injections were performed via a transvitreal approach under isoflurane gas anesthesia. A 44-gauge cannula (Corneal) connected to a viscous fluid injection (VFI) system (D.O.R.C. International, Netherlands) was used to deliver a controlled and automated injection. The cannula was inserted through a sclerotomy and advanced through the vitreous. Under microscopic control, virus solution or vehicle alone (saline) was injected into the subretinal space underlying the tapetal central retina by pressing the VFI system footswitch. Dogs 1 to 3 and 4 to 6 were injected subretinally with 60 to 100 μl of rAAV-2/4.CMV.*gfp* (4×10^{12} vg/ml) or rAAV-2/5.CMV.*gfp* (2×10^{12} vg/ml), respectively, in the right eye. Postsurgical treatment included subcutaneous

FIG. 4. Nonhuman primate model. Live retinal fluorescence imaging at different time intervals (14, 21, 35, and 60 days p.i.) in Mac 1 (A, C, E, G, and I) and in Mac2 (B, D, F, H, and J). Both individuals received rAAV-2/4.CMV.*gfp*. (★) Retinal detachment created by the subretinal injection (A, B). Two months p.i., neuroretina (K, L, and N) and choroid/RPE (M) flat mounts were performed and examined under inverted fluorescence microscope. M, macula; ONH, optical nerve head; RV, retinal vessel.

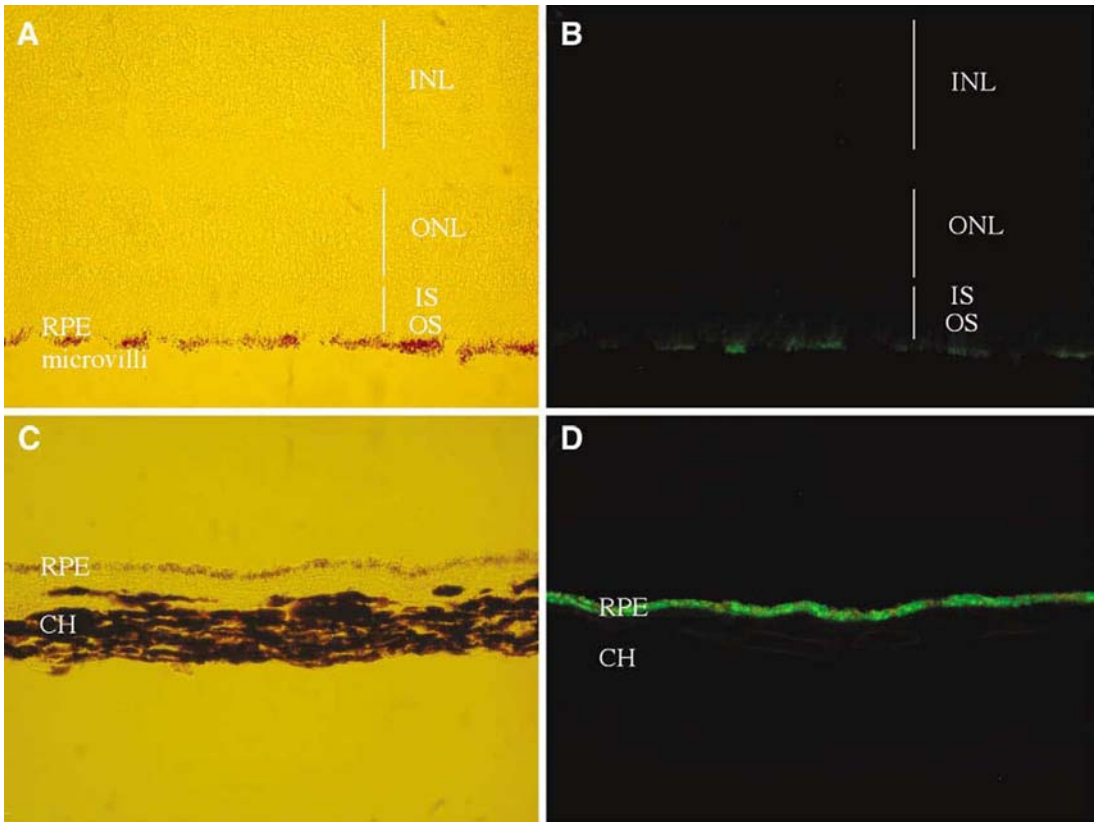

FIG. 5. Nonhuman primate model. Sections from neuroretina (A and B) and choroid/RPE (C and D) flat mounts were analyzed by either normal light microscope (A and C) or inverted fluorescence microscope (B and D). See legend to Fig. 1 for RPE, ONL, INL, and GCL.

injections of Marbocyl (marbofloxacine; 20 mg in 0.2 ml) or Tolfedine (tolferamic acid; 40 mg in 1 ml) and oral administration of Megasolone (prednisolone; 10 mg) for 6 days postsurgery. A vitrectomy was performed in two macaques—Mac1 and Mac2—before the subretinal injection of 40 and 120 μl of rAAV-2/4.CMV.*gfp*, respectively.

In vivo GFP fluorescence imaging, retina flat mounting, and tissue sections. GFP expression in live rats, dogs, and primates was monitored at weekly intervals by retinal fluorescence imaging as described [45]. The sclera/choroid/RPE and neuroretina flat mounting was performed on 4% paraformaldehyde-fixed enucleated eyes as previously described [45]. Tissue sections were also made. For dogs and primates, RPE/choroid layers were separated from the sclera.

Detection of rAAV vector DNA in body fluids after subretinal delivery in dogs and macaques. Biological samples and PCR analyses were processed as previously described [31]. The 5′ primer (5′-AAGTTCATCTGCACCACCG-3′) and the 3′ primer (5′-TGTTCTGCTGGTAGTGGTCG-3′) were both located in the *gfp* DNA sequence. PCR-amplified vector sequence yielded a 424-bp fragment. After initial denaturation at 95°C for 5 min, 40

TABLE 1: Detection of rAAV vector sequences by PCR in body fluids

		Serum	Lacrymal	Nasal	Urine	Feces
Dogs, AAV-2/5	D1	2–14 d	15 m–2 d	15 m–2 d	n.d	n.d
	D2	2–19 d	15 m–1 d	2 d	n.d	n.d
	D3	2–23 d	15 m–3 d	2 h–4 d	n.d	n.d
Dogs, AAV-2/4	D4	1–14 d	15 m–1 d	15 m–1 d	n.d	n.d
	D5	2 h–14 d	15 m–2 d	2 h–1 d	n.d	n.d
	D6	15 m–25 d	15 m–3 d	15 m–2 h	n.d	n.d
Mac, AAV-2/4	Mac1	2 h–16 d	15 m–2 h	15 m–2 h	Negative	Negative
	Mac2	Negative	15 m–2 h	Negative	Negative	Negative

d, days p.i.; h, hours p.i.; m, minutes p.i.; n.d, not done.

doi:10.1016/S1525-0016(03)00098-4

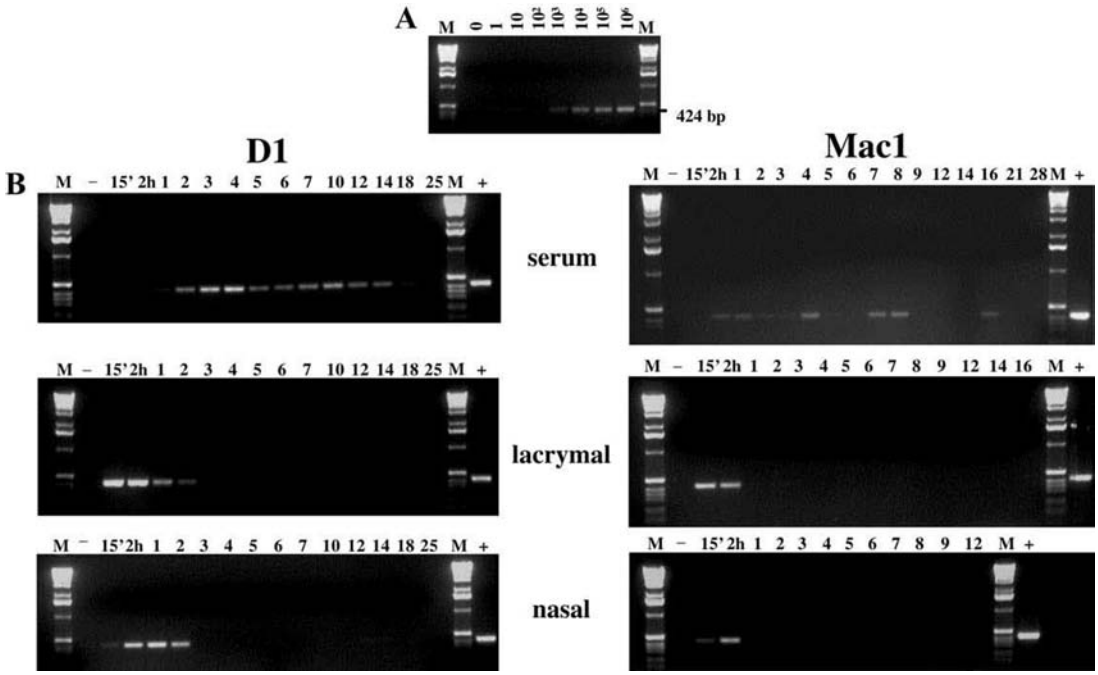

FIG. 6. Vector shedding after subretinal delivery of rAAV-2/4.CMV.*gfp* in dog (D1) and nonhuman primate (Mac1). (A) PCR assay for sensitivity. (B) Serum, lacrymal, and nasal samples are represented. Lanes M, DNA marker; +, positive control on 25 pg of vector plasmid; −, negative control on water. Samples were collected 15 min, 2 h, and day 1 to day 28 p.i.

cycles were run at 94°C for 30 s, 60°C for 30 s, 72°C for 30 s, followed by incubation at 72°C for 10 min using *Taq* DNA polymerase (Promega) in a Perkin–Elmer thermocycler (Perkin–Elmer, USA). Amplified products were analyzed by agarose gel electrophoresis.

ACKNOWLEDGMENTS

We thank the Vector Core of the University Hospital of Nantes (www.vectors.nantes.inserm.fr), supported by the Association Française contre les Myopathies, for the production of the rAAV-2/4.CMV.gfp vector. Fabienne Rolling, Delphine Briot, and this work were supported by a sponsored research agreement from PrimeBioTech. This work was also supported by the French Lions Club and the Lions Clubs International Foundation, the Foundation pour la Thérapie Génique en Pays de la Loire, and INSERM.

RECEIVED FOR PUBLICATION FEBRUARY 11, 2003; ACCEPTED MARCH 6, 2003.

REFERENCES

1. Bohl, D., Bosch, A., Cardona, A., Salvetti, A., and Heard, J. M. (2000). Improvement of erythropoiesis in beta-thalassemic mice by continuous erythropoietin delivery from muscle. *Blood* **95:** 2793–2798.
2. Bosch, A., Perret, E., Desmaris, N., and Heard, J. M. (2000). Long-term and significant correction of brain lesions in adult mucopolysaccharidosis type VII mice using recombinant AAV vectors. *Mol. Ther.* **1:** 63–70.
3. Daly, T. M., Vogler, C., Levy, B., Haskins, M. E., and Sands, M. S. (1999). Neonatal gene transfer leads to widespread correction of pathology in a murine model of lysosomal storage disease. *Proc. Natl. Acad. Sci. USA* **96:** 2296–2300.
4. Elliger, S. S., Elliger, C. A., Aguilar, C. P., Raju, N. R., and Watson, G. L. (1999). Elimination of lysosomal storage in brains of MPS VII mice treated by intrathecal administration of an adeno-associated virus vector. *Gene Ther.* **6:** 1175–1178.
5. Jung, S. C., *et al.* (2001). Adeno-associated viral vector-mediated gene transfer results in long-term enzymatic and functional correction in multiple organs of Fabry mice. *Proc. Natl. Acad. Sci. USA* **98:** 2676–2681.
6. Snyder, R. O., *et al.* (1999). Correction of hemophilia B in canine and murine models using recombinant adeno-associated viral vectors. *Nat. Med.* **5:** 64–70.
7. Wang, B., Li, J., and Xiao, X. (2000). Adeno-associated virus vector carrying human minidystrophin genes effectively ameliorates muscular dystrophy in mdx mouse model. *Proc. Natl. Acad. Sci. USA* **97:** 13714–13719.
8. Xiao, X., *et al.* (2000). Full functional rescue of a complete muscle (TA) in dystrophic hamsters by adeno-associated virus vector-directed gene therapy. *J. Virol.* **74:** 1436–1442.
9. Xiao, W., *et al.* (1999). Gene therapy vectors based on adeno-associated virus type 1. *J. Virol.* **73:** 3994–4003.
10. Muramatsu, S., Mizukami, H., Young, N. S., and Brown, K. E. (1996). Nucleotide sequencing and generation of an infectious clone of adeno-associated virus 3. *Virology* **221:** 208–217.
11. Chiorini, J. A., Yang, L., Liu, Y., Safer, B., and Kotin, R. M. (1997). Cloning of adeno-associated virus type 4 (AAV4) and generation of recombinant AAV4 particles. *J. Virol.* **71:** 6823–6833.
12. Chiorini, J. A., Kim, F., Yang, L., and Kotin, R. M. (1999). Cloning and characterization of adeno-associated virus type 5. *J. Virol.* **73:** 1309–1319.
13. Rutledge, E. A., Halbert, C. L., and Russell, D. W. (1998). Infectious clones and vectors derived from adeno-associated virus (AAV) serotypes other than AAV type 2. *J. Virol.* **72:** 309–319.
14. Gao, G., *et al.* (2002). Novel adeno-associated viruses from rhesus monkeys as vectors for human gene therapy. *Proc. Natl. Acad. Sci. USA* **99:** 11854–11859.
15. Chao, H., *et al.* (2000). Several log increase in therapeutic transgene delivery by distinct adeno-associated viral serotype vectors. *Mol. Ther.* **2:** 619–623.
16. Chao, H., Monahan, P. E., Liu, Y., Samulski, R. J., and Walsh, C. E. (2001). Sustained and complete phenotype correction of hemophilia B mice following intramuscular injection of AAV1 serotype vectors. *Mol. Ther.* **4:** 217–222.
17. Davidson, B. L., *et al.* (2000). Recombinant adeno-associated virus type 2, 4, and 5 vectors: Transduction of variant cell types and regions in the mammalian central nervous system. *Proc. Natl. Acad. Sci. USA* **97:** 3428–3432.
18. Zabner, J., *et al.* (2000). Adeno-associated virus type 5 (AAV5) but not AAV2 binds to the apical surfaces of airway epithelia and facilitates gene transfer. *J. Virol.* **74:** 3852–3858.
19. Ali, R. R., *et al.* (1996). Gene transfer into the mouse retina mediated by an adeno-associated viral vector. *Hum. Mol. Genet.* **5:** 591–594.
20. Ali, R. R., *et al.* (1998). Adeno-associated virus gene transfer to mouse retina. *Hum. Gene Ther.* **9:** 81–86.
21. Bennett, J., *et al.* (1999). Stable transgene expression in rod photoreceptors after

recombinant adeno-associated virus-mediated gene transfer to monkey retina. *Proc. Natl. Acad. Sci. USA* **96:** 9920–9925.
22. LaVail, M. M., *et al.* (2000). Ribozyme rescue of photoreceptor cells in P23H transgenic rats: Long-term survival and late-stage therapy. *Proc. Natl. Acad. Sci. USA* **97:** 11488–11493.
23. Liang, F. Q., *et al.* (2001). AAV-mediated delivery of ciliary neurotrophic factor prolongs photoreceptor survival in the rhodopsin knockout mouse. *Mol. Ther.* **3:** 241–248.
24. Ali, R. R., *et al.* (2000). Restoration of photoreceptor ultrastructure and function in retinal degeneration slow mice by gene therapy. *Nat. Genet.* **25:** 306–310.
25. Green, E. S., *et al.* (2001). Two animal models of retinal degeneration are rescued by recombinant adeno-associated virus-mediated production of fgf-5 and fgf-18. *Mol. Ther.* **3:** 507–515.
26. Lau, D., *et al.* (2000). Retinal degeneration is slowed in transgenic rats by AAV-mediated delivery of FGF-2. *Invest. Ophthalmol. Visual Sci.* **41:** 3622–3633.
27. Acland, G. M., *et al.* (2001). Gene therapy restores vision in a canine model of childhood blindness. *Nat. Genet.* **28:** 92–95.
28. Rabinowitz, J. E., *et al.* (2002). Cross-packaging of a single adeno-associated virus (AAV) type 2 vector genome into multiple AAV serotypes enables transduction with broad specificity. *J. Virol.* **76:** 791–801.
29. Auricchio, A., *et al.* (2001). Exchange of surface proteins impacts on viral vector cellular specificity and transduction characteristics: The retina as a model. *Hum. Mol. Genet.* **10:** 3075–3081.
30. Yang, G. S., *et al.* (2002). Virus-mediated transduction of murine retina with adeno-associated virus: Effects of viral capsid and genome size. *J. Virol.* **76:** 7651–7660.
31. Favre, D., *et al.* (2001). Immediate and long-term safety of recombinant adeno-associated virus injection into the nonhuman primate muscle. *Mol. Ther.* **4:** 559–566.
32. Gal, A., *et al.* (2000). Mutations in MERTK, the human orthologue of the RCS rat retinal dystrophy gene, cause retinitis pigmentosa. *Nat. Genet.* **26:** 270–271.
33. Gu, S. M., *et al.* (1997). Mutations in RPE65 cause autosomal recessive childhood-onset severe retinal dystrophy. *Nat. Genet.* **17:** 194–197.
34. Fisher, K. J., *et al.* (1997). Recombinant adeno-associated virus for muscle directed gene therapy. *Nat. Med.* **3:** 306–312.
35. Xiao, W., *et al.* (1998). Adeno-associated virus as a vector for liver-directed gene therapy. *J. Virol.* **72:** 10222–10226.
36. Nathwani, A. C., *et al.* (2001). Factors influencing in vivo transduction by recombinant adeno-associated viral vectors expressing the human factor IX cDNA. *Blood* **97:** 1258–1265.
37. Herzog, R. W., *et al.* (1999). Long-term correction of canine hemophilia B by gene transfer of blood coagulation factor IX mediated by adeno-associated viral vector. *Nat. Med.* **5:** 56–63.
38. Malik, A. K., *et al.* (2000). Kinetics of recombinant adeno-associated virus-mediated gene transfer. *J. Virol.* **74:** 3555–3565.
39. Fisher, K. J., *et al.* (1996). Transduction with recombinant adeno-associated virus for gene therapy is limited by leading strand synthesis. *J. Virol.* **70:** 520–532.
40. Ferrari, F. K., Samulski, T., Shenk, T., and Samulski, R. J. (1996). Second-strand synthesis is a rate-limiting step for efficient transduction by recombinant adeno-associated virus vectors. *J. Virol.* **70:** 3227–3234.
41. Kay, M. A., *et al.* (2000). Evidence for gene transfer and expression of factor IX in haemophilia B patients treated with an AAV vector. *Nat. Genet.* **24:** 257–261.
42. Wagner, J. A., *et al.* (2002). A phase II, double-blind, randomized, placebo-controlled clinical trial of tgAAVCF using maxillary sinus delivery in patients with cystic fibrosis with antrostomies. *Hum. Gene Ther.* **13:** 1349–1359.
43. Kaludov, N., Brown, K. E., Walters, R. W., Zabner, J., and Chiorini, J. A. (2001). Adeno-associated virus serotype 4 (AAV4) and AAV5 both require sialic acid binding for hemagglutination and efficient transduction but differ in sialic acid linkage specificity. *J. Virol.* **75:** 6884–6893.
44. Salvetti, A., *et al.* (1998). Factors influencing recombinant adeno-associated virus production. *Hum. Gene Ther.* **9:** 695–706.
45. Duisit, G., *et al.* (2002). Five recombinant simian immunodeficiency virus (SIV) pseudotypes lead to exclusive transduction of retinal pigmented epithelium in rat. *Mol. Ther.* **6:** 446–454.